#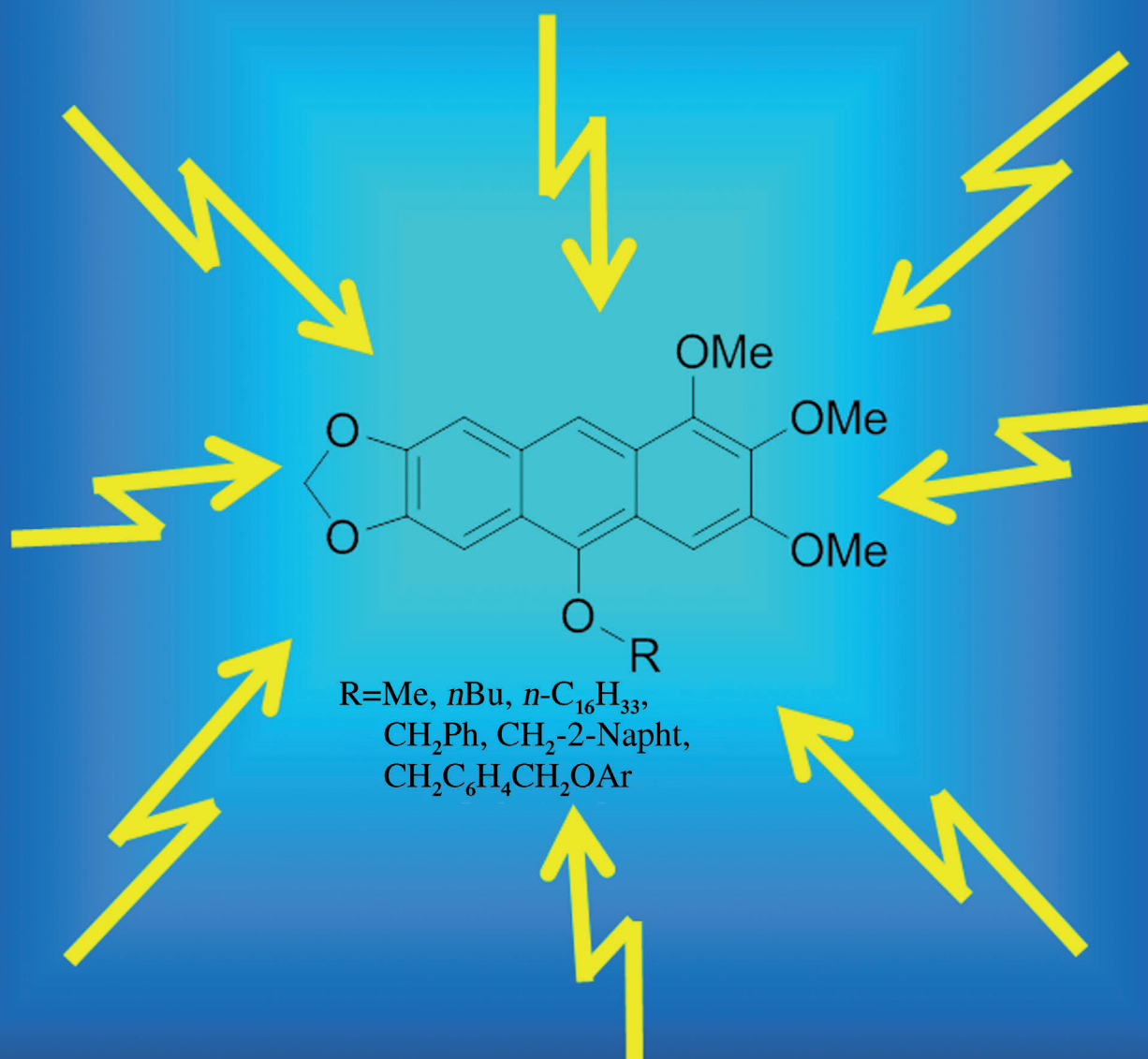 Synthesis and Optoelectronic Properties of Hexahydroxylated 10-*O*-R-Substituted Anthracenes via a New Modification of the Friedel–Crafts Reaction Using O-Protected *ortho*-Acetal Diarylmethanols

Agnieszka Bodzioch,[a] Bernard Marciniak,[b] Ewa Różycka-Sokołowska,[b] Jeremiasz K. Jeszka,[a, d] Paweł Uznański,[a] Sylwester Kania,[c] Janusz Kuliński,[c] and Piotr Bałczewski*[a, b]

Abstract: A new modification of the Friedel–Crafts type intramolecular cyclization involving O-protected *ortho*-acetal diarylmethanols as a new type of reactant, was carried out for the first time in a medium containing a large amount of water at room temperature and enabled synthesis of a series of electron-rich, hexahydroxylated 10-*O*-R-substituted anthracenes, where R is an alkyl (Me, *n*Bu, *n*-C$_{16}$H$_{33}$) or aryl-alkyl group (CH$_2$Ph, CH$_2$-2-Napht, CH$_2$C$_6$H$_4$CH$_2$OAr) and also evaluation of their electronic and optoelectronic properties in solution, crystal, and solid thin film. In this transformation, a central 10-*O*-R-substituted benzene ring was formed, fused to rings originating from two independent aromatic aldehydes. The reaction proceeded via two identified mechanisms involving acetal and/or free aldehyde groups. The acid sensitive acetal and dibenzyl alkoxy functions have never been used together in the intramolecular Friedel–Crafts type cyclization. The new compounds revealed deep blue fluorescence and quantum yields in solution around 0.3. The electrical properties investigated for thin films obtained by vacuum deposition on glass were 10-*O*-R-substituent dependent and showed much faster transient current decay in the case of the 10-*O*-CH$_2$Ph derivative than for the material with a 10-*O*-Me substituent (the lifetime of charge carriers was 25 times shorter in this case). The AFM images of thin films, Stokes shifts, and X-ray analysis of π-stacking interactions in crystals of the new materials have been also obtained.

Keywords: anthracenes · cyclization · fluorescence · Friedel–Crafts · optoelectronic properties

Introduction

Organic electronics and optoelectronics are new fields of basic knowledge and technology which have become a subject of interest to chemists, physicists and process engineers. Therefore a search for organic semiconducting materials for the construction of new generation, electronic devices such as organic light emitting diodes (OLED), organic field-effect transistors (OFET), organic solar cells (OPV), organic solar concentrators (OSC), organic laser etc. has drawn the attention of numerous multidisciplinary joint laboratories. Among fused, polycyclic aromatic hydrocarbons, polyacenes play an important role. Anthracene **1** and its derivatives are particularly attractive due to high thermal stability, relatively good solubility, low price, blue photoluminescent[1] and electroluminescent properties.[2] Many blue-light-emitting materials with the anthracene core structure[3–11] have been developed including one of the best known blue host material, 2-methyl-9,10-di(2,2′-naphthyl)anthracene (MADN).[12] Although a theoretical maximum internal quantum efficiency of nearly 100 % has already been achieved in red and green devices[13] yet the efficiency of deep blue phosphorescent OLEDs is not good enough for commercialization[14] and therefore is a reason of further exploration.

In this paper, we report the synthesis, optical and electrical properties of a series of 10-*O*-R protected (R = Me, *n*Bu, *n*-C$_{16}$H$_{33}$, CH$_2$Ph, CH$_2$-2-Napht, CH$_2$C$_6$H$_4$CH$_2$OAr) anthracene systems **3a–f**, as highly substituted and electron-rich analogues of 9-methoxyanthracene **2** showing a deep blue fluorescence (Scheme 1).

The new anthracenes were obtained by the intramolecular electrophilic substitution reaction operating on O-protected *ortho*-acetal diarylmethanols. These compounds possessed two chemical functions: acetal as the source of an active carbocation and dibenzylalkoxy, which have never been used together in this type of the intramolecular Friedel–Crafts type cyclization, carried out for the first time in a strongly carbocation solvating medium containing a large amount of water under very mild conditions.

In the literature, examples of the Friedel–Crafts type intramolecular cyclization of *o*-formyl,[15] *o*-acyl[16] and *o*-carboxy[17] diarylmethanes and *o*-carboxy[18,19] diarylketones leading to fused, polycyclic aromatic hydrocarbons are known. In this type of reaction, except the first two and our present modification, an additional step involving reduction of intermediate products (anthrone or anthraquinone) is necessary. Moreover, these reactions require harsh reaction conditions (high concentrations of Brønsted acids and high temperature).[20–22] Only a few examples of reactions carried out under mild reaction conditions are known.[23,24] Our modification employs a dilute aqueous methanolic solution (2:1) of hydrochloric acid at room temperature, being the

[a] Dr. A. Bodzioch, Prof. J. K. Jeszka, Dr. P. Uznański, Prof. P. Bałczewski
Department of Heteroorganic Chemistry
Department of Polymer Physics
Department of Engineering of Polymer Materials
Center of Molecular and Macromolecular Studies
Polish Academy of Science
Sienkiewicza 112, 90-363 Łódź (Poland)
Fax: (+48) 426847126
E-mail: pbalczew@bilbo.cbmm.lodz.pl

[b] Dr. B. Marciniak, Dr. E. Różycka-Sokołowska, Prof. P. Bałczewski
Department of Structural and Material Chemistry
Institute of Chemistry, Environmental Protection and Biotechnology
Jan Długosz University
Armii Krajowej 13/15, 42-200 Częstochowa (Poland)

[c] Dr. S. Kania, J. Kuliński
Centre of Mathematics and Physics
Technical University of Łódź
Al. Politechniki 11, 90-924 Łódź (Poland)

[d] Prof. J. K. Jeszka
Department of Man-Made Fibres, Technical University of Łódź
ul. Żeromskiego 116, 90-543 Łódź (Poland)

Supporting information for this article is available on the WWW under http://dx.doi.org/10.1002/chem.201101909.
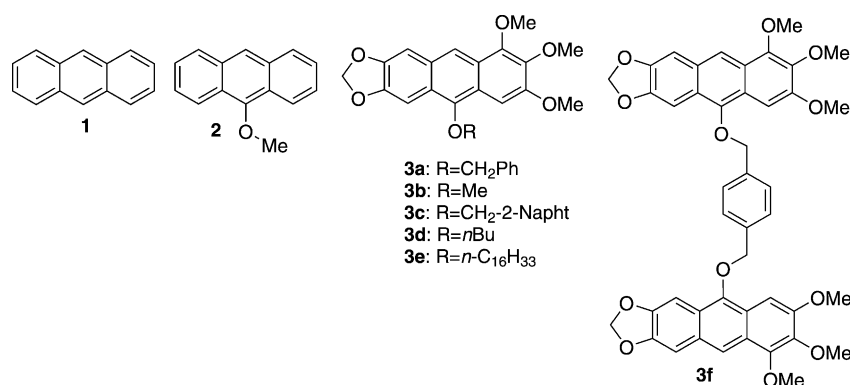
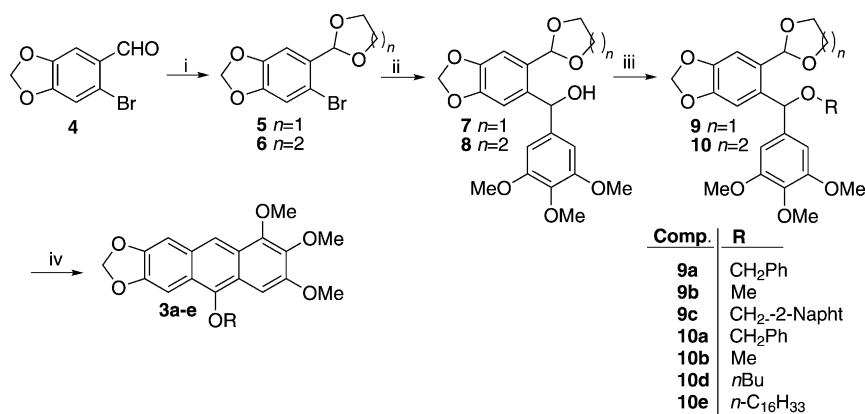Scheme 1. Blue-light emitting anthracenes **3a–f** as examples of functionalized **1** and **2**.

mildest reaction conditions ever used in this type of intramolecular cyclization.[25]

Results and Discussion

Synthesis: The synthesis of a series of 10-*O*-R-substituted anthracene derivatives **3a–e** was based on transformation of 10-*O*-protected *ortho*-acetal diarylmethanols **9** and **10** (Scheme 2). The synthesis of the branched anthracene system **3f** is discussed separately (Scheme 3). The strategy of the synthesis involved: i) protection of the aldehyde group in 6-bromopiperonal **4** with 1,2-ethanediol or 1,3-propanediol to give acetals **5** or **6**, respectively. ii) The Br/Li exchange reaction in **5** or **6** followed by condensation with 3,4,5-trimethoxybenzaldehyde to afford **7** or **8**. iii) protection of the hydroxyl group in **7** or **8** with an alkyl or arylalkyl halide to obtain protected diarylmethanols **9** or **10**, iv) acid-driven cyclization of **9** or **10** to the corresponding anthracene systems **3a–e** (Scheme 2 and Scheme 3). The last step is a Friedel–Crafts type reaction and resembles its later intramolecular modification known as the Bradsher reaction of *ortho*-acyl diarylmethanes.[26–28] Our modification of this reaction differs from the previous examples in that it employs reactants bearing two functional groups, acetal and dibenzyl alkoxy, which are acid

sensitive and, as mentioned, have not been used together before. Therefore, this modified reaction is much more vulnerable to changes of reaction conditions than its original versions and hence required tuning which is also described below.

The new approach to substituted anthracenes arose from the observation of a different behavior of the *O*-benzyl protected diarylmethanol derivatives **9a** in the presence of 1 N HCl in benzene and methanol in synthesis of lignans.[25,29] We showed that this approach could be extended to other polycyclic aromatic hydrocarbons containing nitrogen atoms like benzo[*g*]quinoline, benzo[*b*]carbazole and pyrido[*b*]carbazole systems.[25,30] Thus, **9a** underwent a selective deacetalization in the presence of 1 N HCl in refluxing benzene to give the aldehyde **11a**. However, when the reaction was carried out in 1 N HCl in aqueous methanol (2:1), the unknown hexahydroxylated anthracene

Scheme 2. Synthesis of the anthracene derivatives **3a–e**. Reaction conditions: i) HO(CH₂)₂OH/*p*-TsOH (cat.), benzene, reflux, 26 h (for **5**) or HO(CH₂)₃OH/*p*-TsOH (cat.), benzene, reflux, 4 h (for **6**). ii) 1) *n*BuLi/*n*-hexanes, THF, −78 °C, 15 min, 2) 3,4,5-trimethoxybenzaldehyde, THF, −78 °C to RT. iii) 1) NaH, THF, RT, 30 min, 2) RX (1.5 equiv), RT, 18 h (RX = MeI, PhCH₂Br, NaphtCH₂Br, *n*BuBr, *n*-C₁₆H₃₃I). iv) 1 N HCl, MeOH, RT, 60 h or 1 N HCl, MeOH, reflux, 12 h (for **3e**).
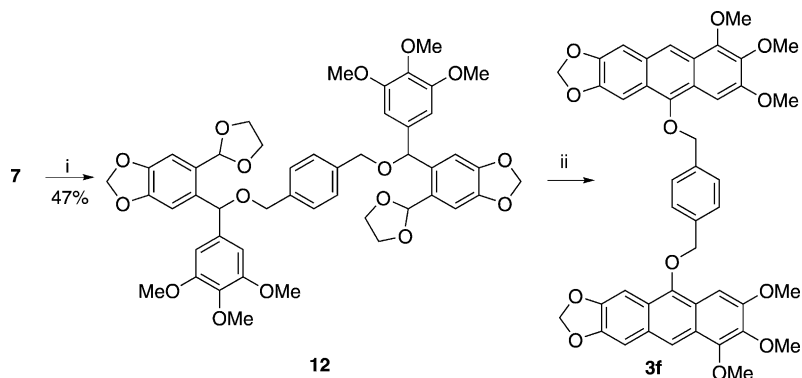
Scheme 3. Synthesis of the anthracene derivative **3f**. Reaction conditions: i) 1) NaH, THF, RT, 30 min, 2) α,α′-dibromo-*p*-xylene, THF, RT, 18 h. ii) 1 N HCl, MeOH, RT, 6 days.

3a was formed unexpectedly in 68% yield (see Scheme 1 in the Supporting Information).

The anthracene **3a** was also formed in case of the 1,3-dioxane protected diarylmethanol derivative **10a**. The similar 53% yield (Scheme 2, Table 1) obtained in this case, suggested that the type of acetal used for protection of the carbonyl function in O-protected *ortho*-acetal diarylmethanols **9** and **10** does not affect the efficiency of the cyclization process. It is worth noting that the 6-membered acetals were formed more easily than their 5-membered analogues and required six times shorter reaction times.
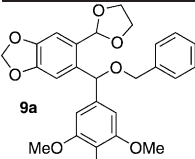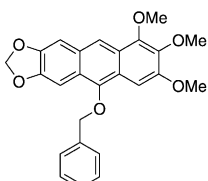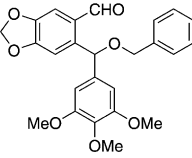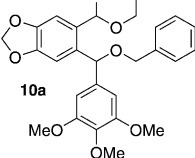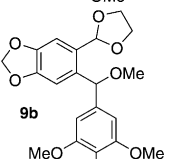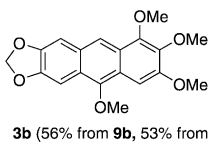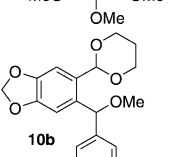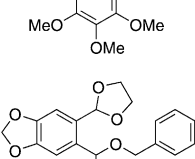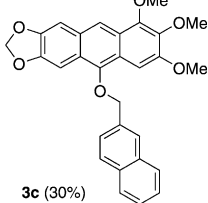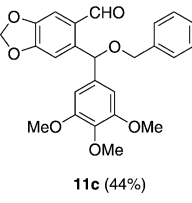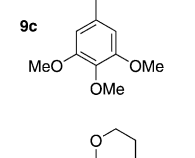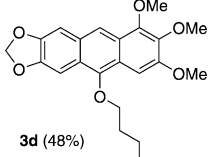
To optimize the conditions for the acid-catalyzed cyclization of **9a** to the anthracene **3a**, we tested a number of acidic reagents, such as Lewis acid, Brønsted acid and strong acidic ion-exchange resins. All the reactions afforded the anthracene **3a** and the aldehyde **11a**, accompanied in some cases by the substrate **9a** and the diarymethanol **7** with a free hydroxyl group (see Table 1 in the Supporting Information).

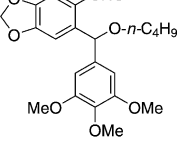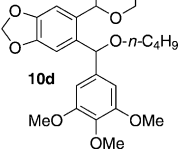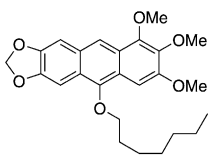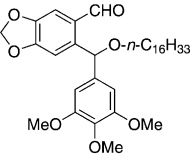Optimized reaction conditions involving aqueous methanol under very mild conditions (1 N HCl, MeOH, RT, 60 h) were applied in this type of the Friedel–Crafts cyclization for the first time. They were next used in the synthesis of the remaining 10-alkoxy (OMe, O-nBu, O-n-$C_{16}H_{33}$) and 10-arylmethoxy (OCH$_2$Ph, OCH$_2$-2-Napht, OCH$_2$C$_6$H$_4$CH$_2$OAr) substituted anthracenes **3b–f**. Unexpectedly, an attempt to transform O-n-hexadecyloxy derivative **10e** to the anthracene **3e** in the presence of 1 N HCl in methanol at room temperature resulted in isolation of the substrate **10e**, accompanied by trace amounts of the corresponding aldehyde **11e**. Finally, refluxing **10e** in methanol in the presence of 1 N HCl afforded after 12 h the desired product **3e** in 38% yield (Scheme 2, Table 1). The key derivatives **9**, **10**, and **12** were obtained by the reaction of diarylmethanols **7** or **8** with alkyl or arylalkyl halides (methyl iodide, n-butyl bromide, n-hexadecyl iodide, 2-(bromomethyl)naphthalene and α,α′-dibromo-p-xylene), (Scheme 2 and Scheme 3, Table 1).

Following our successful synthesis of the series of anthracenes **3a–e** in a single cyclization process, next we prepared bis[(10-anthroxy)methyl]-1,4-benzene derivative **3f**, in which two anthracene molecules are connected via a p-xylene linker, employing in one step two cyclizations, one for each acetal group in **12**. Thus, the reaction

Table 1. The final products: anthracenes **3** and aldehydes **11**, obtained from 1,3-dioxolanes **9** and 1,3-dioxanes **10** under acidic conditions.

Substrates **9** or **10**	Anthracene **3**	Aldehyde **11**
9a / **10a**	**3a** (68% from **9a**, 53% from **10a**)	**11a**
9b / **10b**	**3b** (56% from **9b**, 53% from **10b**)	not isolated
9c	**3c** (30%)	**11c** (44%)
10d	**3d** (48%)	**11d** (28%)
10e	**3e** (38%)	**11e** (21%)

of the diarylmethanol **7** with α,α'-dibromo-*p*-xylene gave the corresponding derivative **12** in 47% yield. Compound **12** in the presence of 1 N HCl was next transformed into bis[(10-anthroxy)methyl]-1,4-benzene derivative **3 f** (Scheme 3). Unexpectedly, compound **3 f** turned out to be very unstable and underwent decomposition during purification by column chromatography. An attempt to purify it by crystallization also led to its degradation. However, a small amount of the pure product **3 f** (15%) isolated by preparative thin layer chromatography (TLC) on silica gel, allowed its unequivocal identification using ^{1}H NMR and MS-EI. This system resembles bis(9-anthroxy)methanes which were reported to be photosensitive below 400 nm due to the high flexibility of the OCH$_2$O spacer.[31] For experimental details, see the Supporting Information.

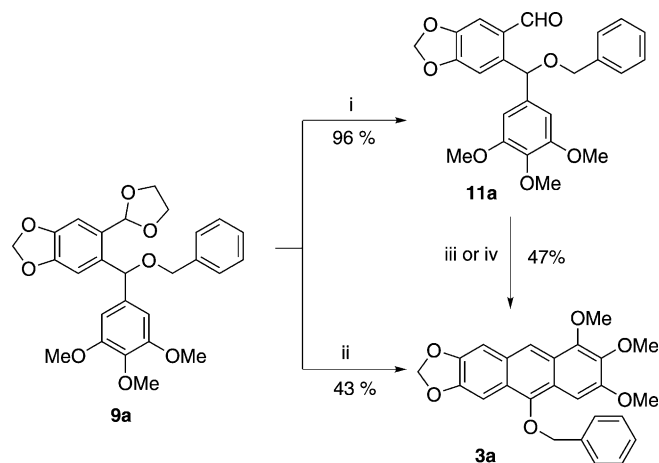Scheme 4. Formation of anthracenes **3** via the aldehyde **11** and/or 1,3-dioxolane **9**/1,3-dioxane **10** mechanistic pathways.

Mechanistic studies and discussion: The mechanism of acid-catalyzed cyclization of diarylmethanol derivatives to anthracene systems proposed previously[29] for the 1,3-dioxolane derivatives can now be extended to 1,3-dioxane analogs and may involve: 1) formation of the benzyl carbocation **13a** as a result of protonation of acetal oxygen, followed by opening of the five- or six membered acetal ring, 2) intramolecular electrophilic Friedel–Crafts-type cyclization combined with formation of the new six-membered ring **14a**, 3) deprotonation and protonation sequence leading to **15a**, 4) elimination of 1,2-ethanediol or 1,3-propanediol from **15**, 5) final aromatization of **16a** to the anthracene **3** (Scheme 4).

Some results obtained during optimization of the cyclization conditions of **9a** to **3a** (See Table 1 in the Supporting Information), especially those obtained for the reaction of **9a** with the ion-exchange resin Amberlyst 15® in acetone, suggested that the above mechanism could operate in parallel with a mechanism of the direct cyclization of diarylmethanols via free aldehydes to anthracenes, as in the Bradsher reaction of *o*-formyl diarylmethanes.[26,27] Thus, the reaction of the diarylmethanol **9a** with Amberlyst 15® in acetone afforded after 4 h the aldehyde **11a** in 96% yield, while after 24 h the anthracene **3a** was isolated in 43% yield (Scheme 5, pathway i and ii). The anthracene **3a** was also the main product of the reaction of the aldehyde **11a** (obtained in an independent way) with Amberlyst 15® in acetone (Scheme 4, pathway iii). In a better cation solvating


Scheme 5. Time dependent transformation of the O-protected diarylmethanol **9a** to the aldehyde **11a** or the anthracene **3a** using Amberlyst 15®. Reaction conditions: i) Amberlyst 15®, acetone, RT, 4 h. ii) Amberlyst 15®, acetone, RT, 24 h. iii) Amberlyst 15®, acetone, RT, 24 h. iv) 1 N HCl, MeOH, RT, 4 days.

aqueous methanolic solution of 1 N HCl, the anthracene **3a** was isolated from **11a** after four days in 47% yield (Scheme 5, pathway iv).

In light of these results, the cyclization mechanism proposed in Scheme 4 can be expanded by the additional possibility of protonation of the aldehyde **11**, and participation of the protonated aldehyde **13b** as the electrophilic species in the first stage of cyclization. Other steps from **14b**–**16** would proceed in an analogous way, and the final stage would involve elimination of water instead of 1,2-ethanediol or 1,3-propanediol (Scheme 5).

Thus, considerations of the mechanism of the above modification of the Friedel–Crafts type cyclization may be reduced to a question of participation in the cyclization of the acetal pathway as an independent step. It seems that this pathway operates, together with the aldehyde pathway, in light of detection of the product **17** ($m/z = 388$, MS-CI) containing a glycol fragment, accompanied by **3a** and **7**, in the reaction of **9a** in the presence of $FeCl_3$ as an acidic catalyst. Similar intermediate compounds **18–20** (Scheme 6), containing 1,3-propanediol fragments were observed by Harvey and co-workers,[32] in the cyclization of triaryl bis-o-acetals, carried out in the presence of a strong acid. Moreover, carbocations **13a** and **13b** which are stabilized in a similar way by resonance, should have similar reactivity in the intramolecular, electrophilic substitution reaction.
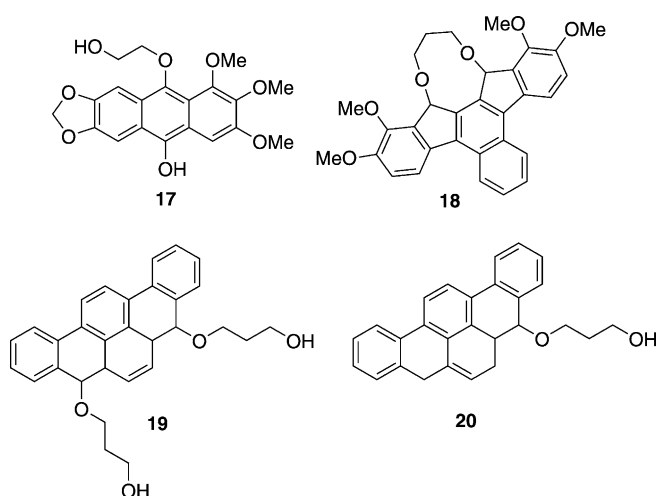
Scheme 6. Intermediate compounds observed in transformations of aryl o-acetals under acidic conditions (**17**: this paper, **18–20**: literature examples).

Crystal and molecular structures of anthracene 3b and anthracene 3d: The compounds **3b** and **3d** crystallized in the monoclinic $P2_1/c$ (Z=4, Z'=1) and triclinic $P\bar{1}$ (Z=2, Z'=1) space groups, respectively. Similarly, as it was observed for anthracene **3a** (CSD[33] refcode ACOTUI[29]), in the case of **3b** and **3d** molecules, anthracene and dioxolane rings as a whole were essentially planar (Figure 1; see the Supporting Information for details).

The crystal structure of **3b** contained two independent weak non-conventional intermolecular C−H···O hydrogen bonds, which individually formed chains of $C(9)$ and $C(10)$ types (Figure 2). The combined effect of these two hydrogen bonds is the formation of a continuous two-dimensional framework, that is, a sheet parallel to (001) and build up from the $R_4^4(34)$ rings (Figure 2). In the crystal structure of **3d**, there were three weak non-conventional intermolecular hydrogen bonds, that is, one hydrogen bond of the C−H···O type and two hydrogen bonds of the C−H···π type. Each molecule was connected to two others by the first interac-
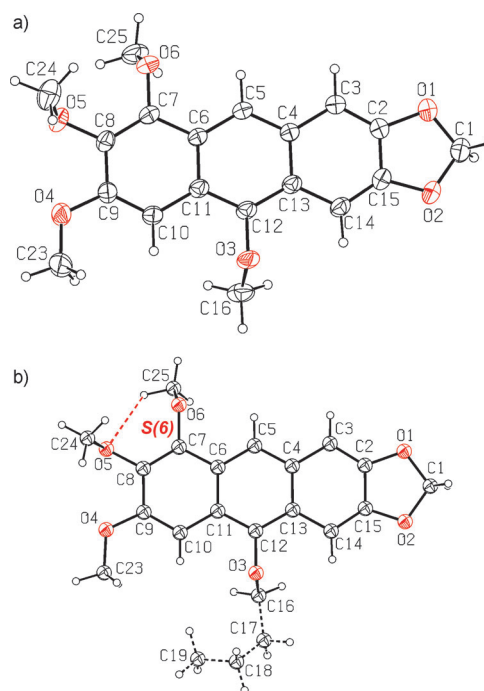
Figure 1. Perspective views of a) **3b** and b) **3d**, showing the atomic numbering schemes. Displacement ellipsoids are drawn at the 30% probability level and H atoms are shown as small spheres of arbitrary radii. The red dashed line in b) denotes the intramolecular C−H···O hydrogen bond, which generates an $S(6)$ graph-set motif.[34]
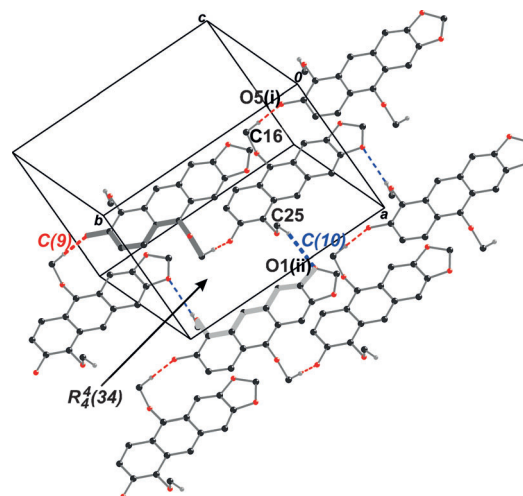
Figure 2. Part of the crystal structure of **3b** showing the (001) sheet built up from $R_4^4(34)$ rings and formed by a combined effect of the two hydrogen-bonded $C(9)$ and $C(10)$ chains running along the crystallographic b axis. The C−H···O hydrogen bonds forming these chains are depicted by red and blue dashed lines, respectively. All hydrogen atoms and the O and C atoms of methoxy groups not involved in the hydrogen-bond motifs have been omitted for clarity. Symmetry codes: (i) $1-x$, $-1/2+y$, $1/2-z$. (ii) $2-x$, $1/2+y$, $1/2-z$.

tion forming a simple $C(8)$ chain, additionally stabilized by one C−H···π hydrogen bond (Figure 3). The molecules belonging to adjacent chains of this type were linked by the second C−H···π hydrogen bond and by the slipped π···π in-

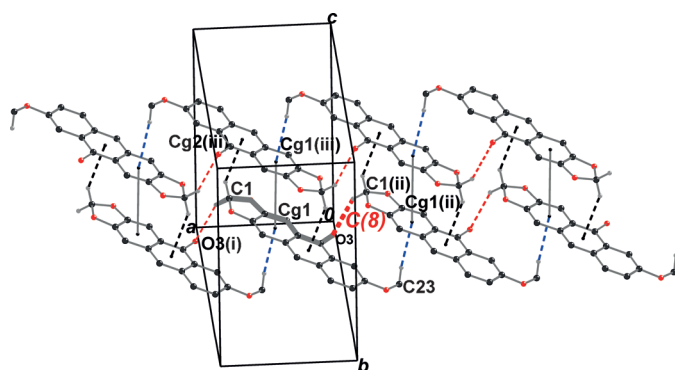Figure 3. Part of the crystal structure of **3d** showing the two antiparallel *C(8)* chains running along the crystallographic axis *a* and formed by the C−H···O and C−H···π hydrogen bonds (red and navy blue dashed lines, respectively). The black dashed and solid lines denote the C−H···π and π···π interactions, respectively, which connect the molecules of adjacent chains. All H atoms, the O and C atoms of methoxy groups and the carbon atoms of butoxy groups not involved in the above interactions have been omitted for clarity. Symmetry codes: (i) 1+x, *y, z*. (ii) 1−x, 1−y, 1−z. (iii) −1+x, *y, z*.
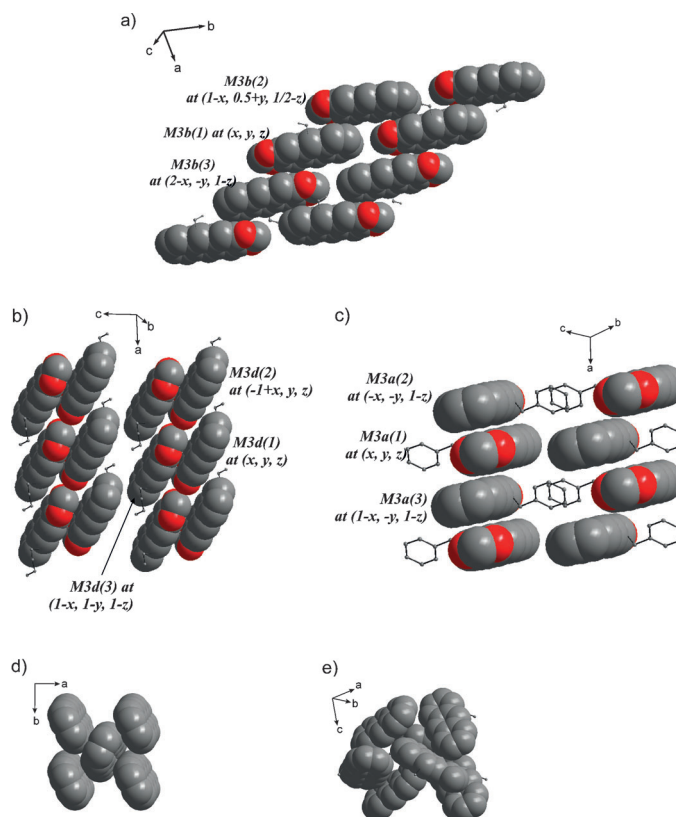

Figure 4. Packing structures of a) **3b**, b) **3d**, c) **3a**, d) **1**, and e) **2**. Columnar stacks of **3b**, **3d**, and **3a**, respectively with a space-filling model for planar moieties, and a ball-and-stick model for the substituents at the 10-position; all hydrogen atoms and carbon and oxygen atoms of substituents at 1-, 2- and 3-positions have been omitted for clarity. d) and e) Herringbone packing diagram of **1** and **2** with the space-filling model (the methoxy substituent in **2** is drawn with the ball-and-stick model; all hydrogen atoms have been omitted for clarity).

teraction (Figure 3). Moreover, it is worth noting that in the crystal structures of **3b**, **3d** and also **3a** there were stacks of parallel in **3d** and **3a** or practically parallel in **3b** anthracene moieties (Figure 4 a–c), without the C−H···π interactions between their rings; these stacks run along the crystallographic axes *a* or the [1̄2̄1̄] direction, respectively (see the Supporting Information for details).

A comparisons drawn between the crystal structures of **3a**, **3b**, **3d**, and those of their simple analogues, that is, unsubstituted anthracene **1** (CSD refcode ANTCEN[35]) and its derivative **2** (i.e. 9-methoxyanthracene; CSD refcode MXANTR01[36]), and also analysis of the 'pitch' and 'roll' parameters [pitch (P) and roll (R) angles and pitch (dp) and roll (dr) distances] estimated for these five compounds according to the phenomenological approach proposed by Curtis et al.[37] for the description of distortions from an 'ideal' cofacial π stack and the values of the extent of the area overlap of adjacent π-stacked molecules (AO), calculated according to a model proposed by Janzen et al.,[38] led to the conclusions given below. A modification of molecular structures of **1** or **2** by the replacement of three hydrogen atoms at positions 1-, 2-, and 3- and two hydrogen atoms at positions 6- and 7- by three methoxy groups and by a methylene-1,3-dioxy unit, respectively, results not only in an elim-

ination of intermolecular C−H···π (arene) interactions between the benzene rings of the anthracene cores, but primarily in a transformation of their arrangement, from typical herringbone in **1** and **2** (Figure 4 d and e; *P* < *R*, *dp* < *dr*) to the parallel or practically parallel stacking in **3b**, **3d**, and **3a** (Figure 4 a–c; *P* > *R*, *dp* > *dr*; Table 2). Moreover, a comparison of the AO values (Table 2) estimated for **3a**, **3b**, and **3d**, that is, for the compounds belonging to the new group of derivatives of 1,2,3-trimethoxy-6,7-(methylene-1,3-dioxy) anthracene possessing a substituent at the 10-position, allowed us to conclude that the extent of the area overlap be-

Table 2. π-Stacking distances (*d*; the shortest distance between the planes of anthracene moieties belonging to the two adjacent molecules (M) in the stack), pitch (*P, dp*) and roll (*R, dr*) parameters and area overlaps (AO) for compounds **3b**, **3d**, and **3a**.

Compound	Pair of molecules in the stacks		*d*	*P*	*R*	*dp* [Å]	*dr* [Å]	AO [%]
3b	M**3b**(1), M**3b** (2)	stack parallel to the [1̄2̄1̄] direction	2.768	62.71	15.58	5.34	0.77	9.4
	M**3b**(1), M**3b**(3)		3.863	59.13	24.98	6.46	1.80	1.5
3d	M**3d**(1), M**3d**(2)	stack parallel to the axis *a*	3.369	61.7	50.53	6.26	4.09	–
	M**3b** (1), M**3d**(3)	between stacks	3.465	62.4	10.10	6.63	0.62	2.9
3a	M**3a**(1), M**3a**(2)	stack parallel to the axis *a*	3.834	60.94	34.75	6.90	2.66	0.1
	M**3a**(1), M**3a**(3)		3.494	49.45	47.24	4.08	3.78	–

[a] Excited at 355 nm. [b] Fluorescence quantum yields (φ_F) were determined by using anthracene (φ_F = 0.29 in benzene) as the standard.[45]

tween anthracene cores in the stacks of molecules depends mainly on the nature of this substituent. Bearing in mind that materials yielding π stacking with substantial spatial overlap in the solid state are particularly attractive because they often lead to devices with high charge carrier mobilities[39–42] and taking into account the fact that in the crystal structure of **3b** such π stacking is predominant, it is possible to suppose that of the group of derivatives, compound **3b** will turn out to be the most promising material for device applications, particularly in the area of functional devices such as organic field-effect transistors (OFETs). This supposition found a confirmation in the results obtained from investigations of optoelectronic properties of the synthesized compounds (for more crystallographic details, see the Supporting Information).

Photophysical properties in solution: UV/Vis absorption spectra of benzoxy (**3a**), methoxy (**3b**), butoxy (**3d**), and hexadecoxy (**3e**) substituted anthracene derivatives are shown in Figure 5. The corresponding fluorescence spectra
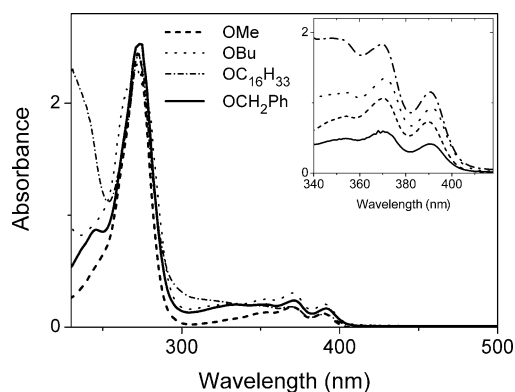
Figure 5. Absorbances of anthracenes **3a** (OCH$_2$Ph), **3b** (OMe), **3d** (OBu), and **3e** (OC$_{16}$H$_{33}$) in CH$_2$Cl$_2$ solution. The inset shows magnification of the long wavelength absorption (absorbance in a.u. for clarity).

are presented in Figure 6 and the positions of maxima, fluorescence quantum yields (Φ$_F$) and Stokes shifts are listed in Table 3. It can be seen that (except for **3b**) neither the in-
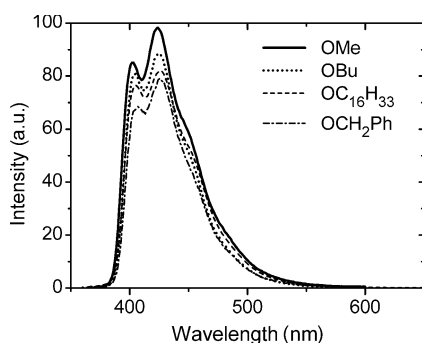
Figure 6. Fluorescence of anthracenes **3a** (OCH$_2$Ph), **3b** (OMe), **3d** (OBu), and **3e** (OC$_{16}$H$_{33}$) in CH$_2$Cl$_2$ solution.

Table 3. UV/Vis absorption and fluorescence properties of **3a**, **3b**, **3d**, and **3e** in CH$_2$Cl$_2$ solution.

Compound	Absorption λ_{max} [nm]	Fluorescence λ_{max} [nm][a]	ϕ_F[b]	Stokes shifts [cm^{-1}]
3a	331, 368, 391	399, 424	0.26	513
3b	354, 370, 389	402, 424	0.32	813
3d	359, 369, 389	401, 424	0.29	769
3e	270, 369, 390	405, 425	0.27	950

[a] Excited at 355 nm. [b] Fluorescence quantum yields (ϕ_F) were determined by using anthracene ($\phi_F = 0.29$ in benzene) as the standard.[45]

crease of the alkyl chain length of the substituted group nor its exchange to phenyl group lead to marked differences with respect to peaks shape and spectral positions, which are determined mostly by the anthracene core. Only a small shift and a change of relative intensities of the maxima for the longest wavelengths are observed.

The quantum yield of fluorescence (Φ_F) calculated in CH$_2$Cl$_2$ solution for methoxy **3b**, butoxy **3d**, benzoxy **3a**, and hexadecoxy **3e** substituted anthracene derivatives oscillated around the 0.3 value (Table 3) and were comparable with the values determined for the unsubstituted anthracene **1** ($\Phi_F = 0.27$[43]) and 1,4,5,8-tetraalkylsubstituted anthracenes ($\Phi_F = 0.25$–0.36, alkyl = Me, Et, *n*Pr, *n*Bu[44]). These results indicate that both the type and position of substituents in the anthracene ring do not affect the value of fluorescence quantum yield in solution.

Photophysical and electrical properties of thin films: Application of organic compounds in molecular electronics requires, in most cases, preparation of thin films. Such films of compounds **3a**, **3b**, and **3d** were prepared by vacuum evaporation (10^{-5} Torr), on glass, spin casting or drop casting. Films of the *O*-Me derivative **3b** crystallized within 2–48 h depending on the film thickness (thin films ca. 1 μm-slowly, thick films ca. 2 μm-quickly). Progress of crystallization of a 2 μm thick film is shown in Figure 7. One can see circular
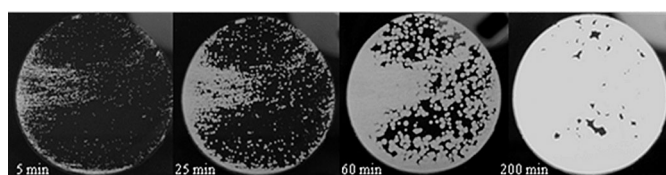
Figure 7. Progress in crystallization of a 2 μm-thick film of the *O*-Me derivative **3b**.

crystalline areas growing in time, which suggests spherulitic growth with primary nucleation on impurities and subsequent secondary nucleation. However, the polarized optical microscope pictures (Figure 8) revealed no preferential orientation of the crystallites.

Figure 8b shows a typical AFM image of such a film and the surface height profile (*z* direction). It can be seen that higher regions of the surface which are probably related to individual crystallites are about 0.7–1 μm long and protrude
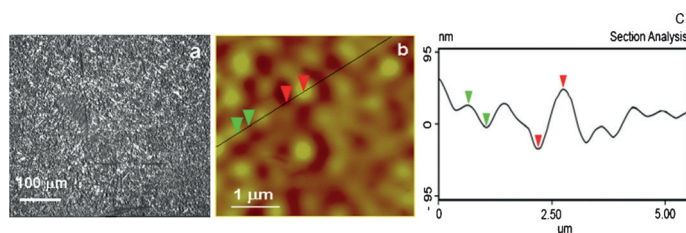
Figure 8. a) Polarized optical microscope picture of 1 μm thick evaporated layer of **3b**. b) AFM image (4 μm), and c) its section analysis along the line indicated on the image.

by 30–80 nm from the surface. The surface roughness (R_{rms}) is 15 nm for the 1 μm film and increases with increasing film thickness, reaching about 78 nm for a 4 μm film. Crystallite size also increases up to about 2 μm.

Films of **3d** obtained in the amorphous state also crystallize after a few days forming crystals of various morphologies (Figure 9), which indicates that this compound can form several polymorphic crystalline structures. Thus less suitable for optoelectronic applications.
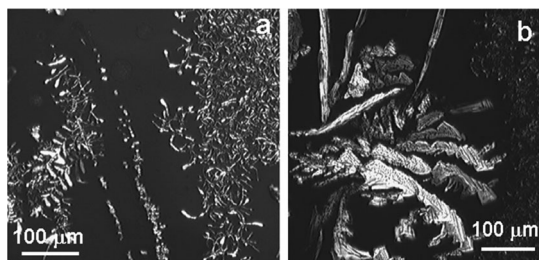

Figure 9. Polarized optical microscope pictures of a semicrystalline dropcast layer of **3d** (after 5 days).

Films of **3a** were obtained by both drop casting and vacuum evaporation, in amorphous form (surface roughness R_{rms} ca. 15 nm). Such layers are stable for at least a couple of weeks but crystallize very slowly, forming after a few months big spherulites with good crystallite orientation and the classical maltese cross image observed under crossed polarizers (Figure 10).

AFM images of the sample surface in amorphous and crystalline forms look similar at first sight but the roughness
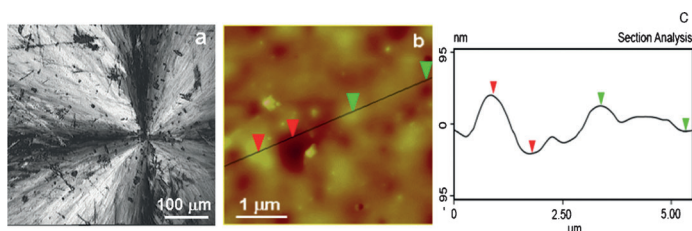

Figure 10. a) Polarized optical microscope picture of the *O*-CH$_2$Ph **3a** (1 μm thick evaporated layer). b) AFM image (height mode) and c) its section analysis along the line shown in Figure 8b. The height differences between the points indicated by triangles are 35 and 75 nm.

of the amorphous layer is of the order of 1.5 nm and it increases to about 11 nm after crystallization.

Absorption spectra in the solid state were recorded for thin layers (below 1 μm), obtained by vacuum evaporation or spin coating (in the case of the *O*-Me derivative **3b**, the spectra were recorded before crystallization of the layer). Low energy maxima, which can be observed are slightly shifted to the blue as compared with the spectra of the same compounds in solution. These data allow us to determine the optical band gaps.

Figure 11 presents the results for the benzoxy **3a**, methoxy **3b**, butoxy **3d** and hexadecoxy **3e** derivatives plotted in appropriate coordinates, assuming that these compounds are direct semiconductors (Tauc plot). Extrapolation of the linear part of the plots to absorption equal to zero gives the value of the optical gap. The obtained band-gaps are: 3.08 eV for **3b** and **3d**, 3.21 eV for **3a**, and 3.10 for **3e** derivatives. A similarity with the corresponding spectra in solution (Figure 5) suggests that in all cases molecular absorption dominates in the solid state and interactions between the molecules are relatively weak. In the case of **3a**, the difference is significant, which suggests that in this case the interactions are relatively strong.
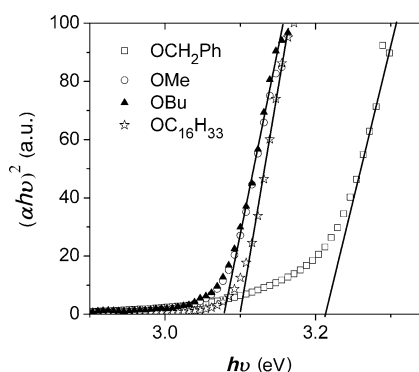

Figure 11. Absorption of the **3a** (*O*-CH$_2$Ph), **3b** (*O*-Me), **3d** (*O*-Bu), and **3e** (*O*-C$_{16}$H$_{33}$) derivatives plotted versus radiation energy to determine the optical band-gap (**3a** and **3b**: evaporated layers, **3d** and **3e**: spin-coated layers).

Figure 12 shows fluorescence emission spectra of compounds **3a**, **3b**, **3d** and **3e** in solution and in the solid state, amorphous and crystalline layers. Crystalline layers were obtained by crystallization of the initially amorphous layers. The emissions of **3b**, **3d**, and **3e** in the crystalline state are similar to those in CH$_2$Cl$_2$ solution (only slightly (14 nm) shifted to the red), which suggests that interactions between these molecules in the solid state are weak.

The fluorescence spectrum thin layers of benzoxy derivative (**3a**; both in amorphous and crystalline state) is exceptionally broad. The band around 540 can be ascribed to formation of excimer centers with relatively strong π-electron interactions between the neighboring molecules. In the crystalline layers such centers are usually related to defects and grain boundaries.[43] In solution, derivatives **3a**, **3b**, and **3d**
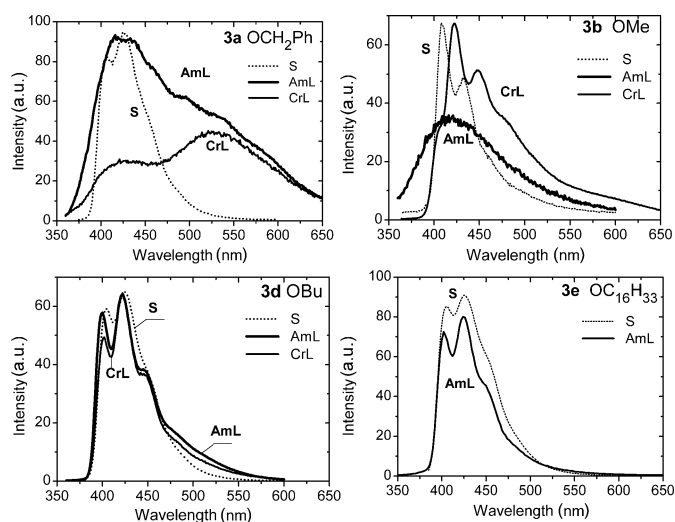
Figure 12. Fluorescence emission spectra of **3a**, **3b**, **3d**, and **3e** derivatives (as indicated in the Figures) in solution (S) and in the solid state: amorphous layer (AmL) and crystalline layer (CrL; vacuum evaporated). Excitation at 350 nm.

do not exhibit marked differences with respect to spectral shape, or the wavelengths of absorption and fluorescence peaks.

Figure 13 shows the time dependence of photoinduced transient currents in the 10-methoxy derivative **3b** layer for
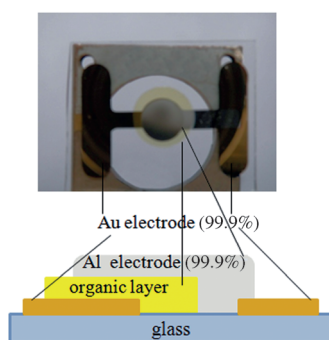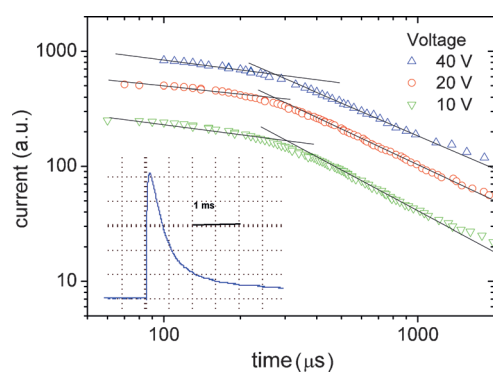

Figure 13. Transient currents time dependence for **3b** plotted in double logarithmic coordinates. The intersection of the two slopes corresponds to the lifetime of photogenerated charge carriers, which is approximately 3 ms. The insert shows a typical oscilloscope trace. The sample thickness was 18.5 μm. A scheme of the investigated device and its picture are shown in the bottom part of the figure.

various voltages plotted in double logarithmic coordinates. The inset shows the oscilloscope trace in linear coordinates. A change of the slope in such plots can be due either to the transit time of the light-induced charge carrier packet (dispersive transport[46] or multiple trapping) or to the life time of charge carriers due to recombination of carriers of opposite signs.[47,48]

As in our case, the time corresponding to the intersection point is practically voltage independent, we can rule out the first possibility. The determined lifetime of charge carriers (holes) is about 200 μs. In the case of derivative **3a** transient currents decay is much faster. The lifetime is of the order of magnitude of the flash lamp pulse so we can only estimate that it is not longer than 7 μs.

Conclusion

In summary, we performed a new approach to 10-*O-R*-substituted anthracenes via acid-catalyzed cyclization of *O*-protected *ortho*-acetal diarylmethanols as a new modification of the Friedel–Crafts reaction. This modification involves acid sensitive acetal and dibenzyl alkoxy groups contained in one molecule and thence requiring special cyclization reaction conditions. The advantage of our protocol over others applied in similar, intramolecular, electrophilic cyclizations, as for instance in the Bradsher reaction (48% HBr in refluxing acetic acid)[25,26] are much milder reaction conditions (1 N HCl, aqueous methanol or acetone at room temperature). This transformation enabled synthesis of a series of blue-light emitting, electron-rich hexahydroxylated anthracenes according to two identified mechanisms. Their full crystallographic structures were determined and π-stacking interactions were analyzed. Optoelectronic properties in solution and solid thin films (absorption and emission spectra, Stokes shifts, fluorescence quantum yields, optical band-gaps, and the life time of charge carriers) were also determined. It was found that the compound **3b** with the best π stacking (as determined by X-ray diffraction) had also the most promising electrical properties due to long lifetime of charge carriers.

Acknowledgements

[1] Y.-H. Kim, D.-C. Shin, S.-K. Kwon, *Adv. Mater.* **2001**, *13*, 1690–1693.

[2] J. Shi, C. W. Tang, *Appl. Phys. Lett.* **2002**, *80*, 3201–3203.

[3] K. H. Lee, J. N. You, S. Kang, J. Y. Lee, H. J. Kwon, Y. K. Kim, S. S. Yoon, *Thin Solid Films* **2010**, *518*, 6253–6258.

[4] Y. Li, M. K. Fung, Z. Xie, S.-T. Lee, L.-S. Hung, J. Shi, *Adv. Mater.* **2002**, *14*, 1317–1321.

[5] B. Balaganesan, W.-J. Shen, C. H. Chen, *Tetrahedron Lett.* **2003**, *44*, 5747–5750.

[6] Y. Kan, L. Wang, Y. Gao, L. Duan, G. Wu, Y. Qiu, *Synth. Met.* **2004**, *141*, 245–249.

[7] Y.-H. Kim, H.-C. Jeong, S.-H. Kim, K. Yang, S.-K. Kwon, *Adv. Funct. Mater.* **2005**, *15*, 1799–1805.

[8] M.-H. Ho, Y.-S. Wu, S.-W. Wen, T.-M. Chen, C.-H. Chen, *Appl. Phys. Lett.* **2007**, *91*, 083515–083517.

[9] Y.-Y. Lyu, J. Kwak, O. Kwon, S.-H. Lee, D. Kim, C. Lee, K. Char, *Adv. Mater.* **2008**, *20*, 2720–2729.

[10] J. K. Park, K. H. Lee, S. Kang, J. Y. Lee, J. S. Park, J. H. Seo, Y. K. Kim, S. S. Yoon, *Org. Electron.* **2010**, *11*, 905–915.

[11] S. E. Janga, C. W. Jooa, K. S. Yooka, J.-W. Kimb, C.-W. Leeb, J. Y. Leea, *Synth. Met.* **2010**, *160*, 1184–1188.

[12] S. W. Wen, M. T. Lee, C. H. Chen, *J. Disp. Technol.* **2005**, *1*, 90–99.

[13] C. Adachi, M. A. Baldo, M. E. Thompson, S. R. Forrest, *J. Appl. Phys.* **2001**, *90*, 5048–5051.

[14] S. O. Jeon, K. S. Yook, C. W. Joo, J. Y. Lee, *Adv. Funct. Mater.* **2009**, *19*, 3644–3649.

[15] M. S. Newman, N. S. Hussain, *J. Org. Chem.* **1982**, *47*, 2837–2840.

[16] M. B. Andrus, Z. Ye, J. Zhang, *Tetrahedron Lett.* **2005**, *46*, 3839–2842.

[17] R. G. Harvey, C. Cortez, T. Sugiyama, Y. Ito, T. W. Sawyer, J. Di-Giovanni, *J. Med. Chem.* **1988**, *31*, 154–159.

[18] J. L. Hallman, R. A. Bartach, *J. Org. Chem.* **1991**, *56*, 6243–6245.

[19] K. L. Platt, F. Oesch, *J. Org. Chem.* **1981**, *46*, 2601–2603.

[20] R. Sangaiah, A. Gold, G. E. Toney, *J. Org. Chem.* **1983**, *48*, 1632–1638.

[21] M. S. Newman, V. S. Prabhu, S. Veeraraghavad, *J. Org. Chem.* **1983**, *48*, 2926–2928.

[22] H. Ihmels, A. Meiswinkel, C. J. Mohrschladt, D. Otto, M. Waidelich, M. Towler, R. White, M. Albrecht, A. Schnurpfeil, *J. Org. Chem.* **2005**, *70*, 3929–3938.

[23] C. K. Bradsher, E. F. Sinclair, *J. Org. Chem.* **1957**, *22*, 79–81.

[24] T. Yamato, N. Sakaue, N. Shinoda, K. Matsuo, *J. Chem. Soc. Perkin Trans. 1* **1997**, 1193–1199.

[25] This reaction was a subject of patent applications: P. Bałczewski, A. Bodzioch, J. Skalik, P-396700, **2011**; P. Bałczewski, A. Bodzioch, J. Skalik, P-389778, **2009**; P. Bałczewski, A. Bodzioch, M. Koprowski, J. Skalik, P-385794, **2008**. (all from the Center of Molecular & Macromolecular Studies PAS, Łódź, Poland).

[26] C. K. Bradsher, *J. Am. Chem. Soc.* **1940**, *62*, 486–488.

[27] C. K. Bradsher, F. A. Vikgiello, *J. Org. Chem.* **1948**, *13*, 786–789.

[28] C. K. Bradsher, *Chem. Rev.* **1987**, *87*, 1277–1297.

[29] P. Bałczewski, M. Koprowski, A. Bodzioch, B. Marciniak, E. Różycka-Sokołowska, *J. Org. Chem.* **2006**, *71*, 2899–2902.

[30] P. Bałczewski, A. Bodzioch, E. Różycka-Sokołowska, B. Marciniak, P. Uznański, *Chem. Eur. J.* **2010**, *16*, 2392–2400.

[31] J. P. Desvergne, M. Gottag, J. C. Soulignac, J. Lauret, H. Bouas-Laurent, *Terrahedron Lett.* **1995**, *36*, 1259–1262.

[32] F.-J. Zhang, C. Cortez, R. G. Harvey, *J. Org. Chem.* **2000**, *65*, 3952–3960.

[33] F. H. Allen, *Acta Crystallogr. Sect. A Acta Crystallogr. B* **2002**, *58*, 380–388.

[34] J. Bernstein, R. E. Davis, L. Shimoni, N.-L. Chang, *Angew. Chem.* **1995**, *107*, 1689–1708; *Angew. Chem. Int. Ed. Engl.* **1995**, *34*, 1555–1573.

[35] C. P. Brock, J. P. Dunitz, *Acta Crystallogr. Sect. A Acta Crystallogr. B* **1990**, *46*, 795–806.

[36] V. Langer, H.-D. Becker, *Z. Kristallogr.* **1993**, *206*, 149–151.

[37] M. D. Curtis, J. Cao, J. W. Kampf, *J. Am. Chem. Soc.* **2004**, *126*, 4318–4328.

[38] D. E. Janzen, M. W. Burand, P. C. Ewbank, T. M. Pappenfus, H. Higuchi, D. A. da Silva Filho, V. G. Young, J.-L. Bredas, K. R. Mann, *J. Am. Chem. Soc.* **2004**, *126*, 15295–15308.

[39] J. E. Anthony, D. L. Eaton, S. R. Parkin, *Org. Lett.* **2002**, *4*, 15–18.

[40] X.-C. Li, H. Sininghaus, F. Garnier, A. B. Holmes, S. C. Moratti, N. Feeder, W. Clegg, S. J. Teat, R. H. Friend, *J. Am. Chem. Soc.* **1998**, *120*, 2206–2207.

[41] G. Horowitz, D. Fichou, D. Yassar, F. Garnier, *Synth. Met.* **1996**, *81*, 163–171.

[42] J. G. Laquindanum, H. E. Katz, A. J Lovinger, A. Dodabalapur, *Adv. Mater.* **1997**, *9*, 36–39.

[43] H. Nakayama, *Chem. Phys. Lett.* **1998**, *289*, 275–280.

[44] C. Kitamura, Y. Abe, N. Kawatsuki, A. Yoneda, K. Asada, T. Kobayashi, H. Naito, *Mol. Cryst. Liq. Cryst.* **2007**, *474*, 119–135.

[45] W. R. Dawson, M. W. Windsor, *J. Phys. Chem.* **1968**, *72*, 3251–3260.

[46] H. Scherr, E. W. Montroll, *Phys. Rev. B* **1975**, *12*, 2455–2477.

[47] H. Fritzsche, *Proc. Int. Summer School on Semiconductors*, ESPOO, Helsinki, **1982**, p. 2.

[48] S. Kania, M. Dłużniewski, *Diamond Relat. Mater.* **2005**, *14*, 74–77.